

# Fabrication of Three-Dimensional Photonic Crystals by Femtosecond Laser Interference

Shigeki Matsuo, Toshiaki Kondo, Saulius Juodkazis, Vyngantas Mizeikis, Hiroaki Misawa  
The University of Tokushima, 2-1 Minamijosanjimacho, Tokushima, Japan

## ABSTRACT

We describe a novel microfabrication method based on interference of several coherent laser pulses in photosensitive media. The method allows to transform the periodic multidimensional interference patterns into periodic modulation of dielectric properties of the material, and is therefore potentially suitable for the photonic crystal fabrication in materials like photoresists, photosensitive glasses, and others. We have fabricated one, two, and three-dimensional photonic crystals with different lattices and sub-micrometer periods. The fabricated structures have high structural quality, as evidenced by confocal and scanning electron microscopies. Furthermore, using numerical simulations we explore the possibilities to obtain body-centered-cubic and diamond photonic crystal lattices by varying optical phases of the interfering beams. Numerical simulations are also used to reveal photonic bandgap properties of some 2D photonic crystals, fabricated using this technique.

**Keywords:** Photonic crystal, laser interference, diffractive beam splitter, femtosecond laser, multi-photon process

## 1. INTRODUCTION

Photonic crystals (PhC) are currently attracting great interest due to their promising applications in integrated optical circuits and low-threshold lasers, etc., as well their role in basic physics.<sup>1-5</sup> Fabrication of PhCs and photonic band gap (PBG) engineering are among the most important tasks. However, fabrication of PhCs which work in the visible or near infrared range is still a challenging topic even with recent progress in micro and nano-technologies. Many techniques have been reported, such as semiconductor fabrication technology,<sup>6-8</sup> organization of microspheres,<sup>9-12</sup> laser microfabrication,<sup>13-15</sup> and their combinations.

The laser interference technique is also applicable for the fabrication of PhCs, because it produces a periodically modulated optical intensity with period comparable to the wavelength. Interference of the two beams creates a one-dimensional (1D) periodic pattern, which is known as a laser-induced grating. A two-dimensional (2D) periodic pattern could be generated by interference of three beams. By using the principle of laser trapping, Burns et al. have demonstrated arrangement of small particles into 2D periodic patterns by interference of laser beams.<sup>16</sup> Three dimensional (3D) periodic patterns also can be fabricated using four or more beams. If such periodic patterns of optical intensity are transferred into the material, PhC can be fabricated. Fabrication of 2D and 3D PhCs by laser interference has been reported by several groups.<sup>17-19</sup> Campbell et al. have made fcc-type 3D PhC structures in photoresist by overlapping four nanosecond pulses.<sup>17</sup> Shoji et al. have fabricated hexagonal PhCs by two-step interference of continuous wave (CW) laser beams.<sup>18</sup>

Recently we have reported fabrication of PhCs using a simple setup based on a diffractive beam splitter (DBS).<sup>19</sup> The simple setup allows us to achieve interference with femtosecond pulses. In addition, interference by many beams, which results in complex periodical structure, is easily achieved with this setup. In this report we describe analysis and fabrication of PhCs by the interference method, and present the PhC structures fabricated using multiphoton absorption.

---

(Send correspondence to S.M. or H.M.)

S.M.: E-mail: matsuos@eco.tokushima-u.ac.jp, fax: 81 (0)88 656 7598, Address: The University of Tokushima, 2-1 Minamijosanjimacho, Tokushima-shi, Tokushima-ken, 770-8506, Japan

H.M.: E-mail: misawa@eco.tokushima-u.ac.jp

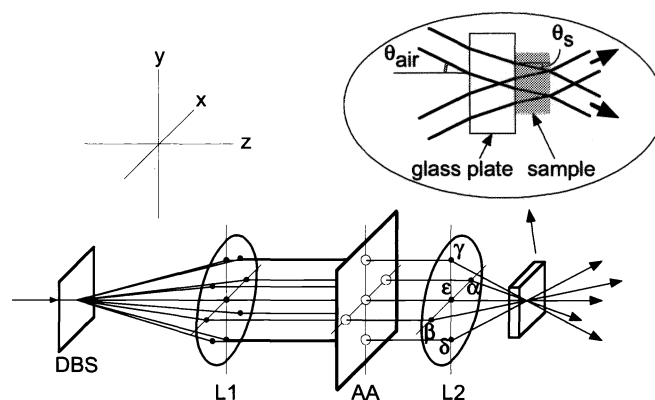


**Figure 1.** Optical setup. DBS is the diffractive beam splitter, L1 and L2 are lenses, and AA is the aperture array. The inset shows beams configuration at the exposure site.

## 2. EXPERIMENT

The optical setup used for the experiments is shown in Fig. 1. The setup essentially consists of a DBS, two lenses, and an aperture array between the two lenses. The DBS splits the introduced laser beam into several components, which are focussed by the lens pair. The aperture array determines the interference pattern by selecting the beams to be interfered. Temporal overlap of femtosecond pulses was achieved without any adjustment of optical path lengths. This is a big advantage of our setup. The details of this setup were described previously.<sup>19</sup> The DBS used in the experiments was G1029A (MEMS Optical, Inc.). It splits the input beam into nine beams. In this study only five of them ( $\alpha$ ,  $\beta$ ,  $\gamma$ ,  $\delta$ ,  $\epsilon$ ) were used, as shown in Figure 1. The angle between the main optical axis ( $z$  axis) and peripheral beams ( $\alpha$ ,  $\beta$ ,  $\gamma$ ,  $\delta$ ),  $\theta$ , which is determined by the DBS, L1, and L2, determines the period of the structure.

Second harmonic of femtosecond pulses from an oscillator (380 nm, 82 MHz) was used as an irradiation source for one-photon absorption fabrication. For the fabrication through multi-photon absorption, femtosecond pulses from a regenerative amplifier (800 nm, 1 kHz) were used. The irradiation power and duration were adjusted to obtain clear periodic structures.

The sample material used to make PhCs was negative photoresist SU-8 (Microlithography Chemical Corp.). Film of SU-8 with a thickness of a few tens  $\mu\text{m}$  was spin-coated on a glass plate, and pre-baked before irradiation. After the irradiation, it was post-baked and developed. Periodic structures were eventually obtained.

For the observation of the fabricated structures, an optical microscope (Olympus IX-70), a scanning confocal microscope (Zeiss LSM-410), and a scanning electron microscope (SEM; Hitachi S-4200SE) were used. For confocal imaging, a small amount of dye (Rhodamine 6G) was added into the photoresist before exposure and luminescence from the dye in the solidified resin was detected. For SEM observation, thin layer of metal (Au) was coated by sputtering.

## 3. RESULTS AND DISCUSSION

### 3.1. Expected Structures: The Effect of Optical Phases

A 2D periodic structure is fabricated by interference of three beams,<sup>20</sup> for example,  $\alpha$ ,  $\beta$ , and  $\gamma$ . Addition of the fourth beam, in general, results in 3D periodic structures.<sup>20</sup> However, since the beams  $\alpha, \beta, \gamma$ , and  $\delta$  have the same wave vector along the main optical axis,  $k \cos \theta$ , where  $k = |\mathbf{k}| = (2\pi/\lambda)$ , interference structures by the four beams should be homogeneous along the main optical axis. As a result, addition of the beam  $\delta$  does not yield 3D periodicity, but can modify the 2D structure.

The total optical intensity profile  $I$  of the interference is calculated as a time-average of the electric field, and the electric field is calculated as a sum of electric fields of plane waves with certain amplitude and phase. The intensity profile of the four beam interference  $I$  is expressed as

$$I = \langle |E_\alpha + E_\beta + E_\gamma + E_\delta|^2 \rangle, \quad (1)$$

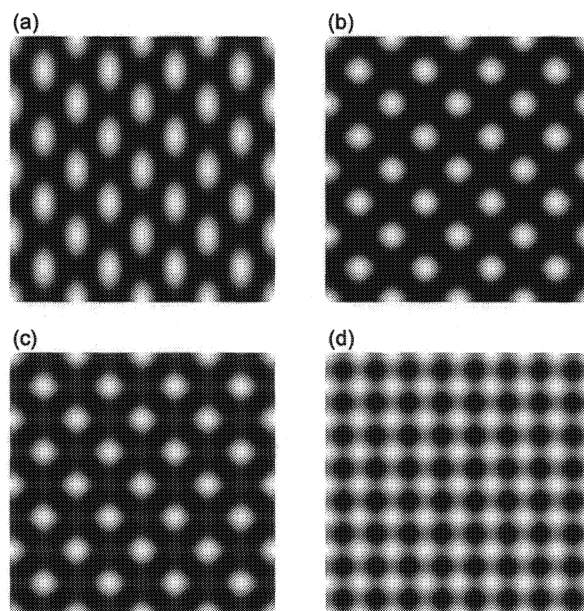


**Figure 2.** Calculated intensity profiles of 2D periodic patterns. (a) by three beams. (b)–(d) by four beams, with different values of parameter  $B$ , (b)  $B = 0$ , (c)  $B = 1/2$ , and (d)  $B = 1$ .

where

$$\begin{aligned}
 E_{\alpha} &= E_0^{\alpha} \cos(C \cdot z - S \cdot x - \omega t + \phi_{\alpha}), \\
 E_{\beta} &= E_0^{\beta} \cos(C \cdot z + S \cdot x - \omega t + \phi_{\beta}), \\
 E_{\gamma} &= E_0^{\gamma} \cos(C \cdot z - S \cdot y - \omega t + \phi_{\gamma}), \\
 E_{\delta} &= E_0^{\delta} \cos(C \cdot z + S \cdot y - \omega t + \phi_{\delta}), \\
 C &= k \cos \theta_s, \\
 S &= k \sin \theta_s,
 \end{aligned}$$

$k$  and  $\omega$  are the wavevector and angular frequency of the beam,  $E_0^i$  and  $\phi_i$  are the electric field amplitude and the phases of the beam  $i$ , respectively. In this case  $I$  is a function of  $x$  and  $y$ , but independent of  $z$ .

At first the intensity profile for a simple case of three beams,  $E_0^i = E_0$  and  $\phi_i = 0$  ( $i = \alpha, \beta, \gamma$ ), and  $E_0^{\delta} = 0$ , is calculated. The intensity profile is

$$I = |E_0|^2 \{2 \cos^2(S \cdot x) + 2 \cos(S \cdot x) \cdot \cos(S \cdot y) + 0.5\}. \quad (2)$$

This is a square lattice shown in Fig. 2 (a). The period (lattice constant) in  $xy$  plane is  $\sqrt{2}\lambda/\sin \theta_s$ .

For a simple case for four beams,  $E_0^{\alpha} = E_0^{\beta} = E_0^{\gamma} = E_0^{\delta} = E_0$  and  $\phi_i = 0$  ( $i = \alpha, \beta, \gamma, \delta$ ), the intensity profile is

$$I = 2 |E_0|^2 \{\cos(S \cdot x) + \cos(S \cdot y)\}^2. \quad (3)$$

This is also a square lattice as described shown in Fig. 2 (b), which has the same lattice constant as Fig. 2 (a) but the shape of each atom is different.

For the three beam interference, change in the optical phases ( $\phi_i$ 's) does not affect the structure, only shifts it as a whole. For the four beam 2D interference, in contrast, the change in optical phase can affect the structure as well as the position of lattice points (but the lattice type is retained). In this case the parameter  $B = \cos((\alpha + \beta - (\gamma + \delta))/2)$  determines the structure.<sup>19</sup> For simplicity of the calculation, suppose that  $\alpha = \beta = -\gamma = -\delta$ . Then, the lattice points do not shift, but the structure changes. The above calculation shown in Fig. 2 (b) is the case of  $2\alpha = 0$

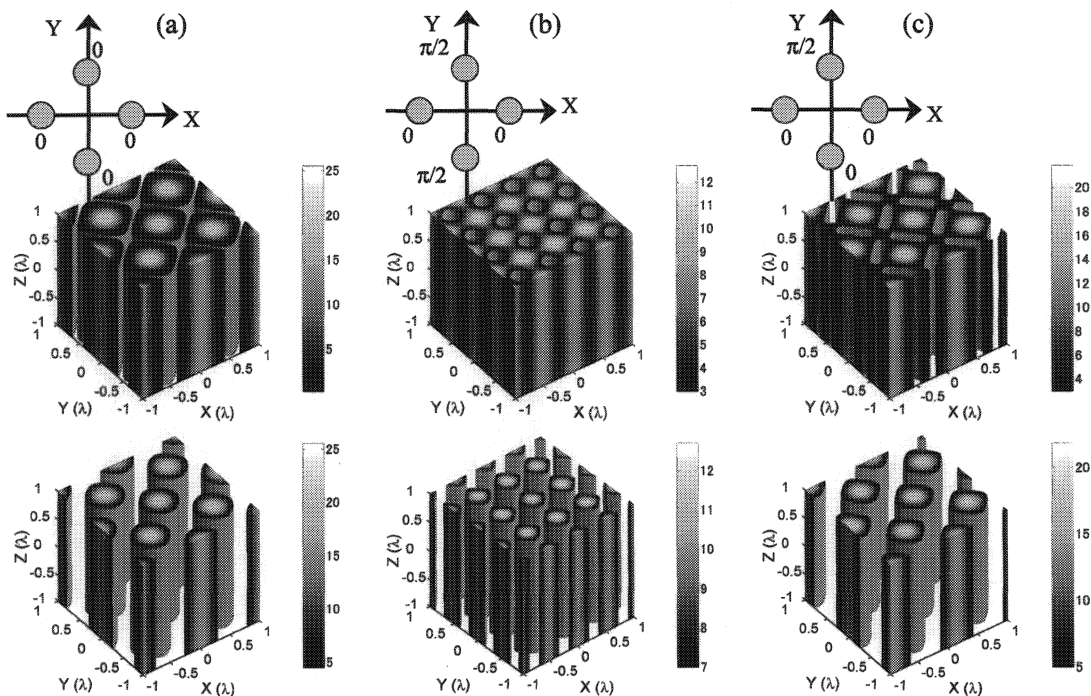


**Figure 3.** Calculated 3D intensity distribution for 4-beams interference. Filled circles schematically depict the beams used for calculations. The electric field amplitude of each beam was 1 and the phases are shown for three different cases (a–c). In the figure, the region where the intensity is lower than a threshold is “washed out”. Top row holograms were calculated for lower threshold and corresponded to a cross-linked structures (except (a)), while the bottom row shows higher threshold patterns, not cross-linked. The angle of each beam with z axis was taken  $\theta = 69^\circ$  for calculations.

(i.e.,  $B = 1$ ). The structures for  $2\alpha = \pi/3$  ( $B = 1/2$ ) and  $2\alpha = \pi/2$  ( $B = 0$ ) are plotted in Fig. 2 (c) and (d), respectively. As seen in Fig. 2 (c), new small peaks appear at the center of the former peaks. This can be regarded as di-atomic structure of the square lattice. Furthermore, the new peaks become of the same height as the former peaks in Fig. 2 (d). Then the structure is still a square lattice but the density of the lattice points is doubled, or the lattice constant is  $1/\sqrt{2}$ .

Similar discussion also applies for 3D periodic structures. By adding the beam  $\epsilon$  to the three or four beams discussed above, we obtain 3D periodic structures. For the case of  $\{\alpha, \beta, \gamma\}$  plus  $\epsilon$ , the structure is body-centered tetragonal. For the beams  $\{\alpha, \beta, \gamma, \delta\}$  plus  $\epsilon$ , the structure varies with relative optical phase from body centered tetragonal to elongated (tetragonal) diamond structure. In the case of uniform  $\phi_i$ 's ( $i = \alpha, \beta, \gamma, \delta$ ), the expected structure is body-centered structure. With a change in phase, again, new lattice points appear, and finally the structure becomes diamond structure. It should be stressed, that a diamond structure could be fabricated through such a simple procedure. Diamond structure is one of the most promising PhC structure for the full photonic bandgap, but difficult to fabricate. Thus, the presented method is useful even if the refractive index of photo-sensitive material is fairly low.

### 3.2. Expected Structures: The Effect of Threshold

Fabrication of real 3D structures requires that they must be self-supporting, i.e., lattice points are interconnected. Since fabrication involves the material's response, which is in general nonlinear and occurs above certain threshold intensity, this factor must be taken into account.

We present simulated 3D light intensity distributions, which were implemented for the negative photoresist exposures. The total intensity is calculated as a sum of the defined number of plane waves with certain amplitude and phase. The most simple 2D structures can be fabricated by using 3- or 4-beams exposure, when only the

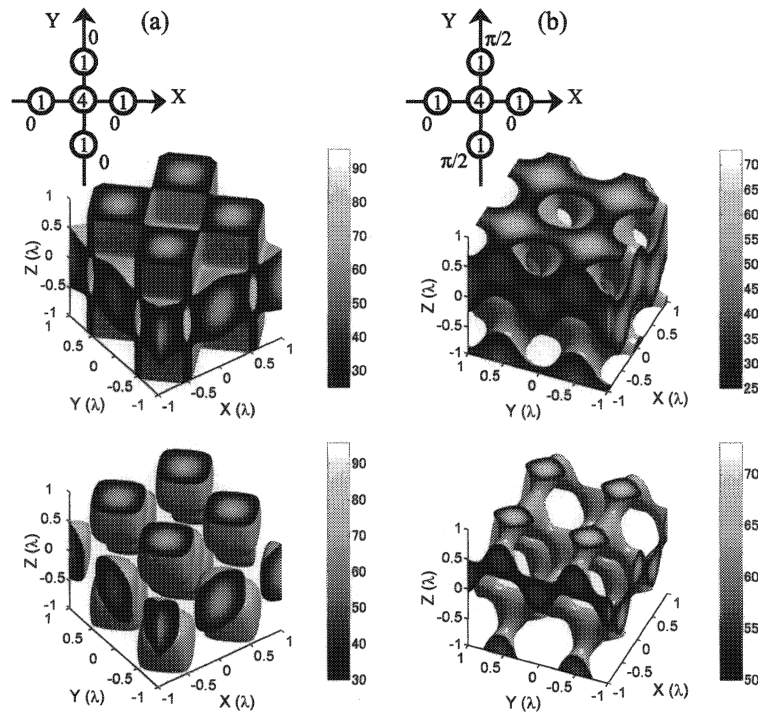


**Figure 4.** Calculated 3D intensity distribution for 5-beams interference. The electric field amplitudes of beams are shown inside and the phases outside the circles (a–b). Top row holograms were calculated for lower threshold and corresponded to the cross-linked structures, while the bottom row shows higher threshold patterns. Conditions and beams geometry were the same as for calculations presented in Fig. 3.

peripheral (without a central) beams are selected (Fig. 1). For an exposed structure to survive the development procedure it is necessary for it to be well cross-linked (self-supporting). For the prospective photonic applications it is important to fabricate structures with the largest possible dielectric contrast (discussed in Sec. 3.4). This puts a requirement on the fabrication not to overexpose the resist in order to be able to remove the largest possible amount of unexposed film. Clearly, these two requirements for self-supporting structures and to removal of large volumes of the unexposed film are contradictory, and the fabrication may become somewhat complicated. Several calculations are presented in Fig. 3 (2D periodic structures) and Fig. 4 (3D periodic structures). In Fig. 4 it is interesting that the neighboring lattice points tend to connect in the structure (b) (diamond structure) rather than structure (a) (body centered structure).

The real spatial intensity profile of the beams used in the fabrication is another relevant topic. In order to maximize the area of uniformly formed structure in the resist the hat-top intensity distribution would be the most favorable.

### 3.3. Fabricated Structures

Several periodic structures by one-photon absorption have already presented.<sup>19</sup> Here, structures by multi-photon absorption (MPA) at 800 nm exposure are presented. SEM images are shown in Fig. 5 for an increasing exposure time (a)-to-(c). Holographic fabrication through MPA have been reported by several authors,<sup>21–26</sup> but they were only two-beam interference, as a result the periodicity was one dimensional. Our method enabled spatial and temporal overlap of four (even more) femtosecond pulses, and fabrication of multi-dimensional periodic structures through MPA.

The rod-like structures in Fig. 5 were recorded over the entire thickness of the resist film, which was about 4  $\mu\text{m}$ . MPA would facilitate an increase in the spatial resolution of the fabricated structures, since the photo-modification of resist follows the  $I^2$  law, where  $I$  is the intensity of light. However, such fine structures are easily washed out through a development process, thus an increase in spatial resolution is still not clear in the structures of Fig. 5.

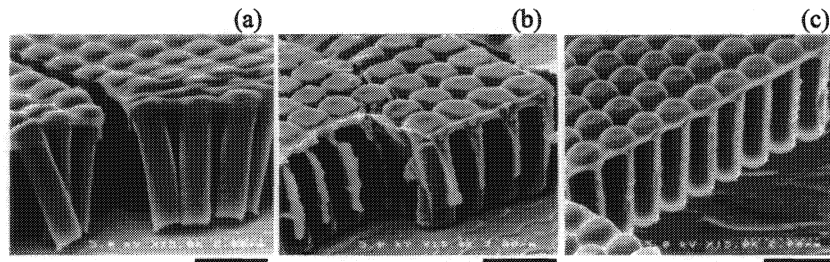


**Figure 5.** SEM images of fabricated structures by 4-beams (the peripheral beams were used, no central beam) exposure at 800 nm wavelength. Exposure time at 1 kHz repetition rate was 30 s (a), 80 s (b), and 120 s (c), respectively. The focusing of beamlets corresponded to  $\theta = 42^\circ$ . Scale bars, 2  $\mu\text{m}$ .

### 3.4. Expected Structures and Optical Properties

As the material in previous sections demonstrates, the interferometric recording is potentially very powerful technique for the fabrication of periodic dielectric structures in resin. Ultimately this potential has to be tested in practice by producing PhC structures with an observable PBG effect. The most crucial problem encountered on this path is relatively low refractive index of the solid resin  $n = 1.67$  compared to  $n = 1$  of air. The low refractive index contrast prevents formation of the PBG. As it was shown in numerous theoretical works, even for the optimum lattice geometries it is impossible to achieve PBG if the refractive index contrast is lower than approximately 2 to 1.<sup>27,28</sup> In such structures only a weaker pseudogap can result. Just as the PBGs, pseudogaps are recognized from dips (peaks) in the PhC transmission (reflection) spectra. However, the transmitted (reflected) intensity variation in the pseudogap spectral region is still below one in at least one direction. Thus, in PhCs in resin one can expect to observe only photonic pseudogaps. To the best of our knowledge, successful practical test of such kind has not yet been reported in literature. Below we will present numerical simulations which examine in qualitative terms the expected optical signatures of photonic pseudogaps in the PhC structures discussed in this work.

All of the 2D periodic structures shown in Fig. 3 have square space lattice, which is determined by two mutually perpendicular primitive translation vectors, and a lattice period  $a$ . The two vectors and the lattice period define an infinite square grid. A periodic dielectric structure can be constructed by placing one or several uniformly arranged dielectric discontinuities (i.e., “atoms”) at each node of the grid. As can be easily seen by examining various plots in Fig. 3, most of the “atoms” are fairly similar to nearly-cylindrical or nearly-square dielectric rods, or cylindrical holes in a dielectric. For the simplicity of our qualitative simulations we did not try to reproduce these shapes exactly, but have chosen several PhC structures built from square or cylindrical dielectric elements with appropriately chosen sizes (defined by ratio between the cylinder radius  $r$  or square side  $w$ , and the lattice period  $a$ ). The results of the transfer-matrix calculations are shown in Fig. 6. The plots in Fig. 6 (a) approximately correspond to the structures shown in the bottom of Figs. 3 (a) and (b). In the case of relatively large ( $r/a = 0.35$ ) dielectric cylinders broad stop bands are observed in both  $\langle 10 \rangle$  and  $\langle 11 \rangle$  directions, but in the latter case the dip transmission for TE polarized light does not reach zero. This finding is in agreement with the well-established trend of TE gaps being more weakly pronounced than TM ones in PhCs consisting of isolated dielectric elements (i.e., cylinders) with higher refractive index.<sup>2</sup> By comparing the transmission spectra in the  $\langle 10 \rangle$  and  $\langle 11 \rangle$  directions it can be also seen that the transmission dips shift significantly, leaving no overlap between these two directions. Altogether, these findings indicate that although no complete PBG can be expected on PhCs with similar parameters, quite significant transmission dips, signifying photonic stop bands, can be expected. The plots in Fig. 6 (b) approximately represent the square-drilled dielectric structure shown in the top of Fig. 3 (b). For relatively small holes ( $r/a = 0.2$ ), regions of higher refractive index are interconnected, thus favouring the formation of TE gaps. This is clearly illustrated by the transmission spectra along the  $\langle 11 \rangle$  direction, where TM gap transmission does not fall to zero. Just as in the previous case, large spectral shift between different directions indicates that full PBG cannot develop. The spectra in Fig. 6 (c) correspond most closely to the top plot in Fig. 3 (a) and the bottom plot in Fig. 3 (c). For the PhC crystals consisting of isolated dielectric square rods with  $w/a = 0.3$ , the transmission within each individual dip goes down to zero, but lack of the spectral overlap between different propagation directions and polarizations makes it impossible to achieve the PBG. Finally, it must be noted that since the structure shown at the top in Fig. 3 (c) is a more complex interconnected network of square rods with two different sizes, our simple calculations cannot be applied for it. However, it will

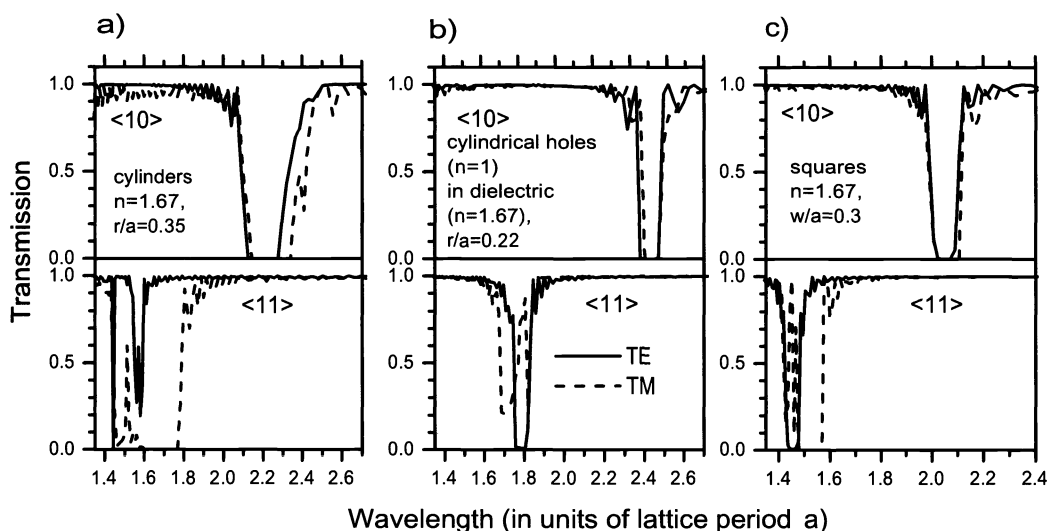


**Figure 6.** Calculated transmission spectra of various prototype 2D PhC structures with square lattice, recorded in resin, (a) for dielectric cylinders, (b) for cylindrical holes in dielectric, (c) for square dielectric rods. The refractive index of the dielectric  $n = 1.67$ , the ratios  $r/a$  and  $w/a$  define radius  $r$  of the cylinders and width  $w$  of the squares with respect to the lattice period  $a$ . The wavelength in the plots is normalized to  $a$ . TE and TM denote two orthogonal linear polarizations of the electromagnetic waves, with the TE polarization being parallel to the rods/cylinders. The propagation direction labelled  $\langle 10 \rangle$  is along the sides of the primitive square cell, while  $\langle 11 \rangle$  is along its diagonals.

most likely not produce to a transmission spectra, qualitatively different from those obtained and discussed above.

It is helpful to note here, that the wavelength axis in the plots presented in Fig. 6 is normalized to the lattice constant  $a$ . Such normalization is possible due to the scaleability property of the Maxwell's equations. The calculated images in Fig. 3 indicate that  $a$  may approach half-wavelength of the recording laser pulse. Returning to Fig. 6, one can notice that since all spectral dips occur at the normalized wavelengths from 1.5 to 2.4, this range will approximately correspond to the range from 0.7 to 1.2 of the recording wavelength (in absence of other limiting factors). Thus it follows, that the pseudogap central wavelength and the fabricating laser wavelength are about equal under these circumstances. The most important remaining question is how to turn the photonic pseudogap into the full PBG. One of the solutions is to look for resins which have higher refractive index. Another solution is to use the fabricated resin structures as templates for in-filling by other high refractive index materials. Both of these options are potentially interesting for the future research.

#### 4. SUMMARY

We have demonstrated a laser interference method for the fabrication of PhC structures based on diffractive beam splitter. This method has advantages of simple optical setup, and flexibility in structure through the choice of interfering beams. 2D periodic PhC structures fabricated through multi-photon process were presented and characterized.

#### REFERENCES

1. E. Yablonovitch, "Photonic band-gap structures," *J. Opt. Soc. Am. B* **10**, pp. 283–295, 1993.
2. J.D. Joannopoulos, R.D. Meade, and J.N. Winn, *Photonic Crystals*, Princeton University Press, Princeton, 1995.
3. K. Sakoda, *Optical Properties of Photonic Crystals*, Springer, New York, 2001.
4. Technical Digest of PECS2001 and references therein.
5. V. Mizeikis, S. Juodkazis, A. Marcinkevicius, S. Matsuo, and H. Misawa, "Tailoring and characterization of photonic crystals," *J. Photochem. Photobiol. C: Photochem. Rev.* **2**, pp. 35–69, 2001.

6. S.Y. Lin, J.G. Fleming, R. Lin, M.M. Sigalas, R. Biswas, and K.M. Ho, "Complete three-dimensional photonic bandgap in a simple cubic structure," *J. Opt. Soc. Am. B* **18**, pp. 32–35, 2001.
7. S. Noda, K. Tomoda, N. Yamamoto, and A. Chutinan, "Full three-dimensional photonic bandgap crystals at near-infrared wavelengths," *Science* **289**, pp. 604–606, 2000.
8. S. Noda, M. Yokoyama, M. Imada, A. Chutinan, and M. Mochizuki, "Polarization mode control of two-dimensional photonic crystal laser by unit cell structure design," *Science* **293**, pp. 1123–1125, 2001.
9. A.V. Blaaderen, R. Ruel, and P. Wiltzius, "Template-directed colloidal crystallization," *Nature* **385**, pp. 321–324, 1997.
10. K. Fukuda, H.-B. Sun, S. Matsuo, and H. Misawa, "Self-Organizing Three-Dimensional Colloidal Photonic Crystal Structure with Augmented Dielectric Contrast," *Jpn. J. Appl. Phys.* **37**, pp. L508–L511, 1998.
11. K.H. Lin, J.C. Crocker, V. Prasad, A. Schofield, D.A. Weitz, T.C. Lubensky, and A.G. Yodh, "Entropically driven colloidal crystallization on patterned surfaces," *Phys. Rev. Lett.* **85**, pp. 1770–1773, 2000.
12. Y.A. Vlasov, X.Z. Bo, J.C. Sturm, and D. Norris, "On-chip natural assembly of silicon photonic bandgap crystals," *Nature* **414**, pp. 289–293, 2001.
13. H.-B. Sun, S. Matsuo, and H. Misawa, "Three-dimensional photonic crystal structures achieved with two-photon-absorption photopolymerization of resin," *Appl. Phys. Lett.* **74**, pp. 786–788, 1999.
14. B.H. Cumpston, S.P. Ananthavel, S. Barlow, D.L. Dyer, J.E. Ehrlich, L.L. Erskine, A.A. Heikal, S.M. Kuebler, I.-Y.S. Lee, D. Mccord-Maughon, J. Qin, H. Rökel, M. Rumi, X.-L. Wu, S.R. Marder, and J.W. Perry, "Two-photon polymerization initiators for three-dimensional optical data storage and microfabrication," *Nature* **398**, pp. 51–54, 1999.
15. H.-B. Sun, V. Mizeikis, Y. Xu, S. Juodkakis, J.-Y. Ye, S. Matsuo, and H. Misawa, "Microcavities in polymeric photonic crystals," *Appl. Phys. Lett.* **79**(1), pp. 1–3 (2001).
16. M.M. Burns, J.-M. Fournier, and J.A. Golovchenko, "Optical Matter: Crystallization and Binding in Intense Optical Fields," *Science* **249**, pp. 749–754, 1990.
17. M. Campbell, D.N. Sharp, M.T. Harrison, R.G. Denning, and A.J. Turberfield, "Fabrication of photonic crystals for the visible spectrum by holographic lithography," *Nature* **404**, pp. 53–56, 2000.
18. S. Shoji and S. Kawata, "Photofabrication of three-dimensional photonic crystals by multibeam laser interference into a photopolymerizable resin," *Appl. Phys. Lett.* **76**, pp. 2668–2670, 2000.
19. T. Kondo, S. Matsuo, S. Juodkakis, and H. Misawa, "Femtosecond Laser Interference Technique with Diffractive Beam Splitter for Fabrication of Three-Dimensional Photonic Crystals," *Appl. Phys. Lett.* **79**, pp. 725–727, 2001.
20. A.J. Turberfield, "Photonic crystals made by holographic lithography," *MRS Bulletin* **26**, pp. 632–636, 2001.
21. S.M. Kirkpatrick, J.W. Baur, C.M. Clark, L.R. Denny, D.W. Tomlin, B.R. Reinhardt, R. Kannan, and M.O. Stone, "Holographic recording using two-photon-induced photopolymerization," *Appl. Phys. A* **69**, pp. 461–464, 1999.
22. L.L. Brott, R.R. Naik, D.J. Pikas, S.M. Kirkpatrick, D.W. Tomlin, P.W. Whitlock, S.J. Clarson, and M.O. Stone, "Ultrafast holographic nanopatterning of biocatalytically formed silica," *Nature* **413**, pp. 291–293, 2001.
23. K. Kawamura, T. Ogawa, N. Sarukura, M. Hirano, and H. Hosono, "Fabrication of Surface Relief Gratings on by Two-beam Holographic method using infrared femtosecond laser pulses," *Appl. Phys. B* **71**, pp. 119–121, 2000.
24. K. Kawamura, N. Sarukura, M. Hirano, and H. Hosono, "Holographic Encoding of Permanent Gratings Embedded in Diamond by Two Beam Interference of a Single Femtosecond Near-infrared Laser Pulse," *Jpn. J. Appl. Phys.* **39**, pp. L767–769, 2000.
25. K. Kawamura, N. Sarukura, M. Hirano, and H. Hosono, "Holographic encoding of fine-pitched micrograting structures in amorphous SiO<sub>2</sub> thin films by a single femtosecond laser pulse," *Appl. Phys. Lett.* **78**, pp. 1038–1040, 2001.
26. K. Kawamura, N. Sarukura, M. Hirano, and H. Hosono, "Periodic nanostructure array in crossed holographic gratings on silica glass by two interfered infrared-femtosecond laser pulses," *Appl. Phys. Lett.* **79**, pp. 1228–1230, 2001.
27. K.M. Ho, C.T. Chan, and C.M. Sokoulis, "Existence of photonic gaps in periodic dielectric structures," *Phys. Rev. Lett.* **65**, pp. 3152–3155, 1990.
28. H.S. Sözüer, J.W. Haus, and R. Inguva, "Photonic bands: convergence problems with the plane-wave method," *Phys. Rev. B* **45**, pp. 13962–13972, 1992.